



Study of NACA 0015 for Diffuser Design in Tidal Current Turbine Applications

N. Mehmood^{a*}, Z. Liang^a, J. Khan^b

^a Deepwater Engineering Research Center, Harbin Engineering University, 150001, Harbin, China

^b College of Shipbuilding Engineering, Harbin Engineering University, 150001, Harbin, China

PAPER INFO

Paper history:

Received 16 July 2012

Received in revised form 11 August 2012

Accepted 30 August 2012

ABSTRACT

Tidal energy is the most foreseeable form of renewable energy. Tidal energy can be harnessed by tidal barrage, tidal fence and tidal current technologies. Present efforts are focused on diffuser augmented tidal turbines that exploit the kinetic energy of the tidal currents. Power generated by a tidal current turbine is due to the cubic relationship between power and flow velocity. A minor increase in flow velocity can significantly increase the power output. A diffuser is a device that can help in stimulating flow velocity. Incorporating a diffuser around a turbine can increase the efficiency of the tidal turbine. Many research groups are investing considerable time and financial resources in this emerging domain. Limited results are available for diffuser augmented tidal turbines due to their emerging nature, large and costly research and development setup, startup cost and proprietary issues. The purpose of this paper is to study a NACA 0015 airfoil for diffuser design for tidal current turbines. Numerical simulation of the diffuser is carried out to check the velocity and mass flow rate at throat. The drag, for various NACA 0015 diffuser models is also calculated on the diffuser.

doi: [10.5829/idosi.ije.2012.25.04c.12](https://doi.org/10.5829/idosi.ije.2012.25.04c.12)

1. INTRODUCTION

Tidal energy is one of the oldest forms of energy used by mankind. Tidal energy can be harnessed by capturing potential or kinetic energy of the tides. The conventional method is to build semi permeable barrages across estuaries with a high tidal range to capture potential energy. The alternate option is to capture the kinetic energy of the tidal currents using underwater devices similar to wind turbines. The building of a dam or barrage across estuary, or a tidal bay, is an expensive project. The building of a dam changes the tidal flow and results in negative impact on aquatic and shoreline ecosystem.

In 1929 [1] Betz accepted the significance of ducts around a turbine. In 1950, a Japanese researcher Sanuki [2] came up with a diffuser showing 88% increased power output relative to Betz limit. In 1953, Iwasaki [3] came up with a cylindrical shape diffuser claiming 30% increase in power output. In 1956, British researchers Lilley and Rainbird [4] concluded that the main contributors that can increase power output by placing a diffuser around a turbine are amplified axial flow

velocity and reduction in turbine blade tip losses. In 1950s, Kogan managed to achieve an augmentation factor of 3.5 [5, 6]. Foremann in 1970 [7] started working on DAWT by placing slots to control the boundary layer separation. He concluded that augmentation factor of 3 is possible [8]. In 1977, Lewis [9] concluded that diffuser area ratio plays an important role in diffuser design. After Igara and Foremann, there was renewed interest in exploring DAWT. In 1979, De Varies pointed out that the force a diffuser exerts on the incoming flow governs the DAWT augmentation factor [10]. In 1997, New Zealand based company Vortex made a 17 m tall diffuser augmented wind turbine. Full scale model Vortex 7 was built and measured maximum power coefficient of 0.62 [11].

The horizontal axis tidal turbine is one of the most popular tidal current technologies [12]. The efficiency of a horizontal axis tidal turbine depends on marine current velocity and water depth. The ideal marine current velocity for a horizontal axis tidal turbine is around 2 m/sec. However, the average available marine current velocity around the globe is around 1 m/sec. In order to harness tidal energy at such low velocity, a much bigger turbine system with large turbine diameter is required. However, increasing the turbine diameter

* Corresponding Author Email: thatsnasir@live.com (N. Mehmood)

creates issues, such as the water depth limitation, huge support structure and increased drag on the system. Thus, increase in incoming current velocity is severely needed. This issue is resolved by a diffuser augmented tidal current turbine. The diffuser augmented tidal turbine (DATT), turbine enclosed in a diffuser, is based on the principle that the generated power output by a tidal turbine is directly proportional to the cube of velocity of incoming fluid flow [13]. Thus, even a minor increase in velocity considerably increases the generated power output. The diffuser acts as a flow amplification device by accelerating the incoming flow, hence increasing the mass flow rate and the power output. The turbine inside the diffuser generates the same power output with smaller turbine diameter compared to naked turbine. Consequently, diffuser augmented tidal turbine is more viable economically compared to naked turbines.

The terminologies duct, shroud, diffuser and diffuser augmented tidal turbine are being used interchangeably in the literature, referring to the same concept. Extensive research work is in progress around the world to explore the potential of diffuser augmented turbine to harness more power than open turbine [14-16]. Numerous tidal current turbine designs which incorporate a diffuser have been emerged. There are mainly two types of diffuser configurations as shown in Figure 1 [17]:

(A) Rectilinear shape

- With inlet
- Without inlet
- Without inlet having flange or brim
- With inlet and flange or brim

(B) Annular ring shape

The purpose of this paper is to present numerical simulation of 2D models of diffuser for tidal current turbine. Numerical simulation of the velocity profile at the throat of the diffuser is presented in detail. The effect of length and angle of attack on maximum velocity, average velocity, mass flow rate and drag is discussed. This research serves as foundation for using CFD tools for diffuser design used for tidal current turbines.

2. MODELING OF DIFFUSER AND BOUNDARY CONDITIONS

NACA 0015 airfoil has been used to generate 2D model of the diffuser as shown in Figure 2(a). 3D model of the diffuser is shown in Figure 2(b) for better visualization. Typical components of a tidal turbine along with diffuser is shown in Figure 3(a) and 3(b), respectively.

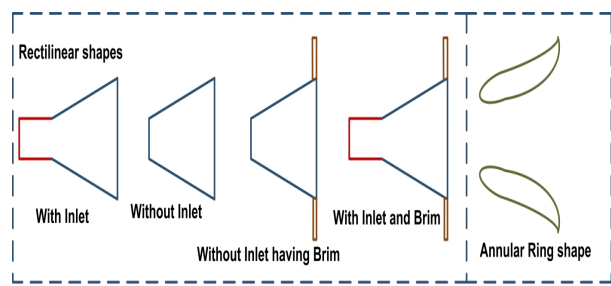


Figure 1. Types of diffuser configurations [17]

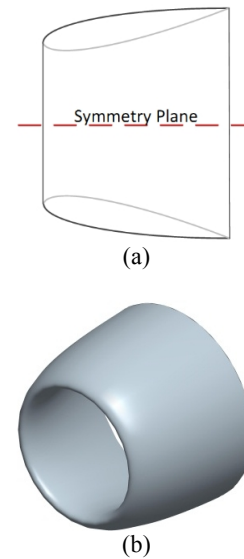


Figure 2. (a) 2D view of the diffuser, (b) 3D model of the diffuser

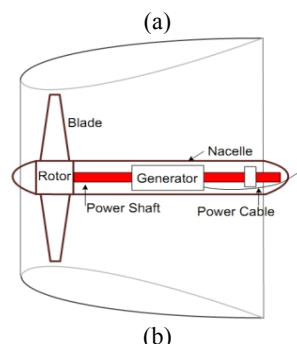
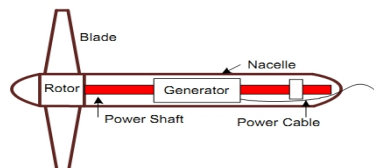


Figure 3. (a) Typical tidal turbine, (b) Turbine enclosed in a diffuser

Modeling has been carried out using MATLAB. After importing the data points in MATLAB, airfoil has been scaled and rotated from the leading edge according to desired values. A parametric study has been undertaken, with the diffuser length at 400, 500, 600, 700, 800, 900, and 1000 mm, and for seventeen angles of attack ranging from 0 to 16 degrees. The diameter of the throat is fixed at 710 mm. Ten monitoring points are created at throat of the diffuser for in-depth analysis and exploration of maximum velocity profile, average velocity and mass flow rate. Drag force on the diffuser, along the X-axis, is also calculated. The schematic view of NACA 0015 airfoil with monitor points at throat is depicted in Figure 4. NACA 0015 airfoil is rotated from the leading edge and is shown in Figure 5.

ANSYS ICEM has been used to create the computational mesh. The domain inlet is 5L upstream of the diffuser with a uniform flow velocity of 1.2 m/sec. The outlet is 10L downstream of the diffuser as shown in Figure 6. Mesh has been generated using Ansys ICEM, the y^+ value is less than 10 for mesh spacing. Meshed domain along with airfoil is shown in Figure 7 and close up view of the meshed airfoil is shown in Figure 8. The simulation has been carried out using commercially available software ANSYS CFX. SST turbulence model has been used due to its superior performance for predicting boundary layer separation with adverse pressure gradient [13,18].

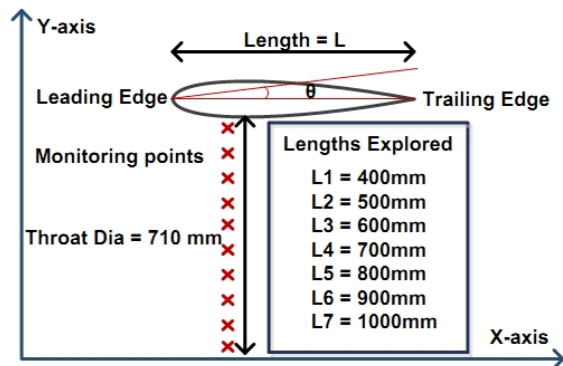


Figure 4. Schematic view of NACA 0015 with monitor points

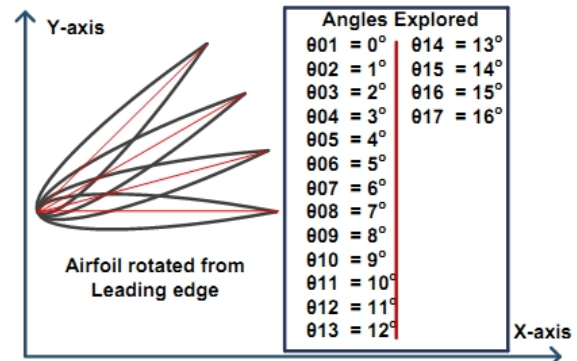


Figure 5. Schematic view of NACA 0015 with angles explored

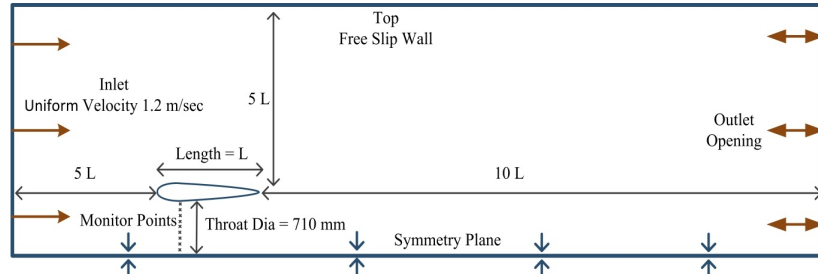


Figure 6. Domain and boundary conditions

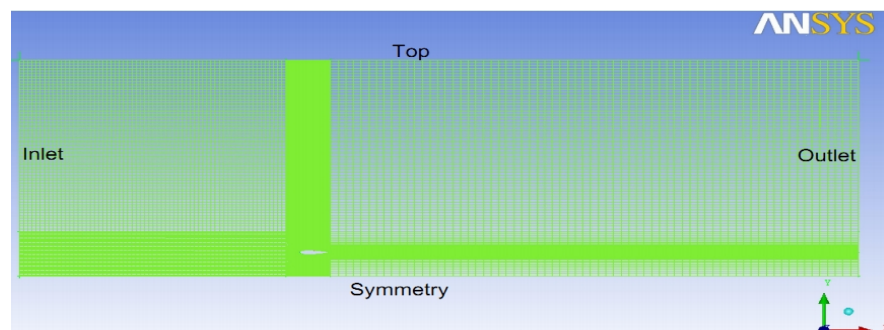


Figure 7. Meshed domain with NACA 0015 airfoil

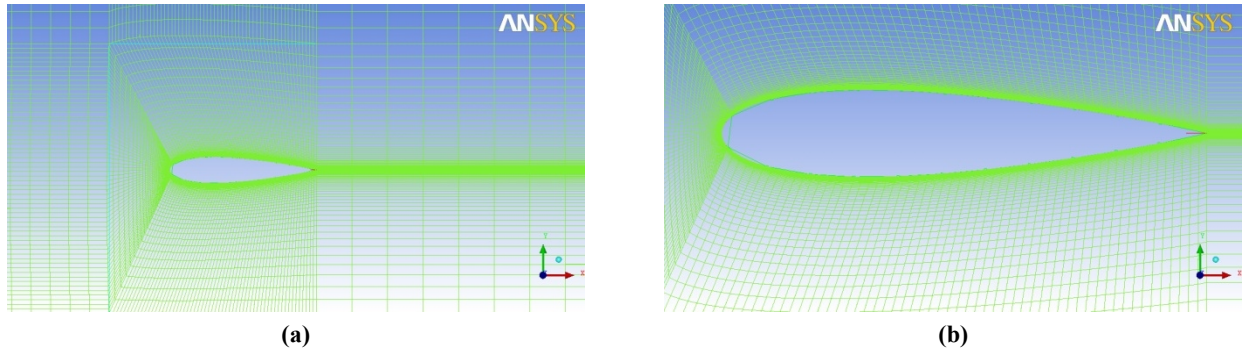


Figure 8. Airfoil mesh in ANSYS ICEM. (b) Close up view of airfoil mesh

3. RESULTS AND DISCUSSIONS

NACA 0015 has been explored at seven different lengths. Every length is explored at seventeen different angles of attack. Mesh convergence study has been carried out on maximum velocity. Ten different densities of mesh are generated to achieve mesh convergence. Figure 9 shows a plot of maximum velocity versus mesh elements showing the change in velocity results for different mesh densities. The simulation has already been validated by comparing the experimental results with simulation results [13].

In Figure 10, the maximum velocity achieved at throat is shown as the angle of attack which is varied from zero degree minimum to 16 degree maximum. There is a gradual increase in maximum velocity from 1.5 m/s to 3.18 m/s. It can be seen that the profile of maximum velocity is almost linear which implies that the velocity increases with length and angle of attack.

The trend of average velocity is shown in Figure 11 where the average velocity is shown at the throat line. Average velocity is taken at ten monitoring points at the throat line. Coefficient of velocity (C_v) is shown in Figure 12. Coefficient of velocity is the ratio of maximum velocity to inlet velocity which is 1.2 m/s. Mass flow rate is the function of velocity and cross sectional area. Figure 13 illustrates mass flow rate at the throat line at different lengths and angles. It has been observed that mass flow rate drops exactly at the same angles where average velocity drops. Coefficient of mass flow rate (C_q) is shown in Figure 14. Coefficient of mass flow rate is the ratio of throat mass flow rate to mass flow rate at inlet of the diffuser.

Drag force, on the diffuser along the X-axis, is also calculated. Direction of flow is along positive X-axis. Figure 15 shows drag force against angle of attack. It is evident that drag also increases with the length and angle of attack. Coefficient of drag is shown in Figure 16. Area ratio is shown against angle of attack in Figure

17. Area ratio is the ratio of diffuser outlet area to throat area.

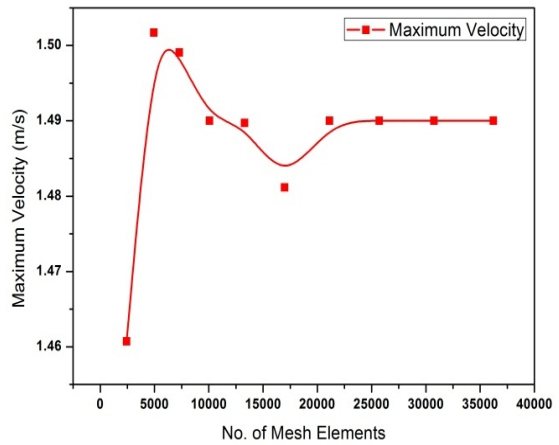


Figure 9. Mesh convergence curve

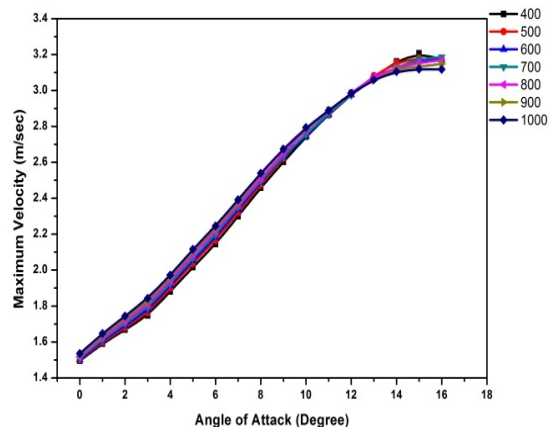
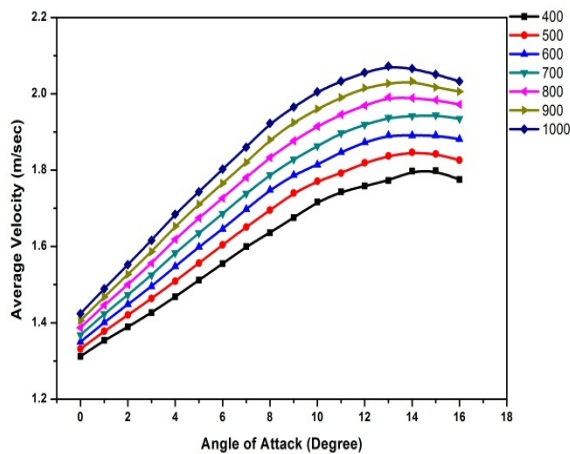
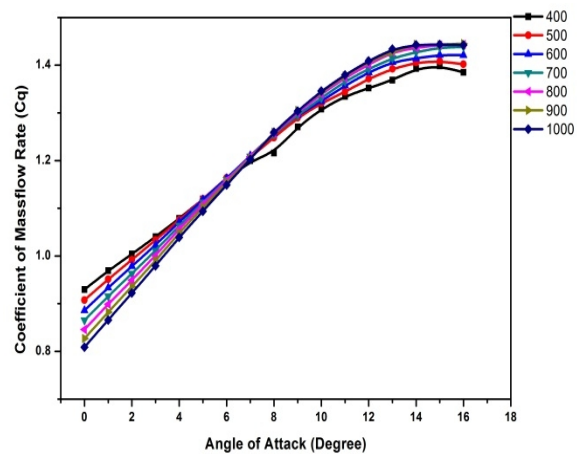
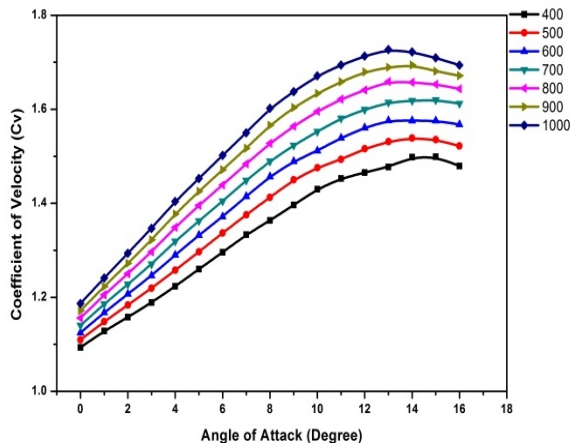
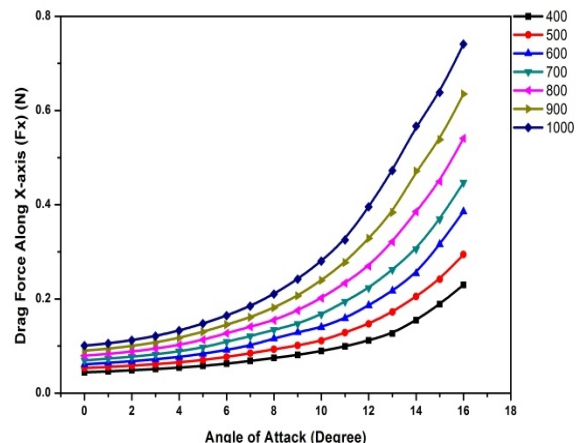
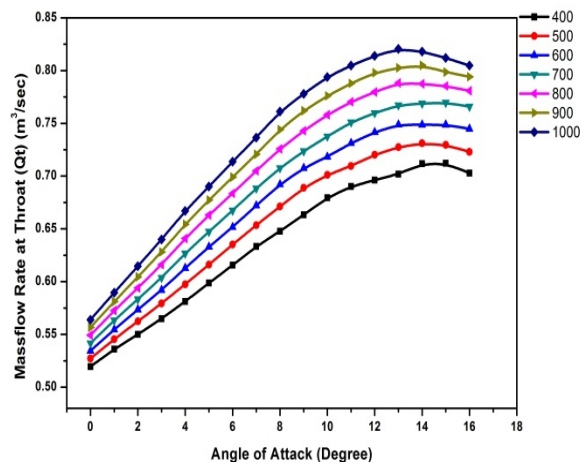
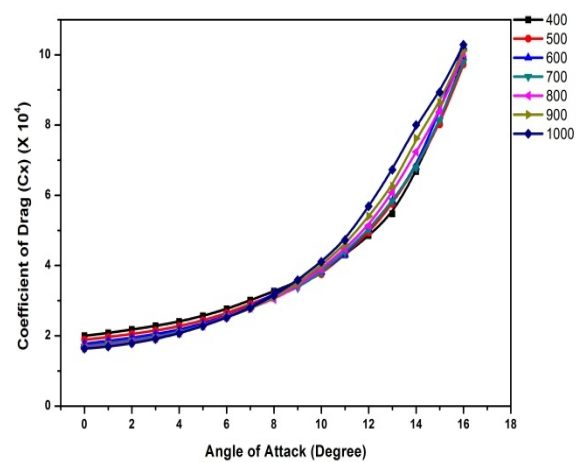
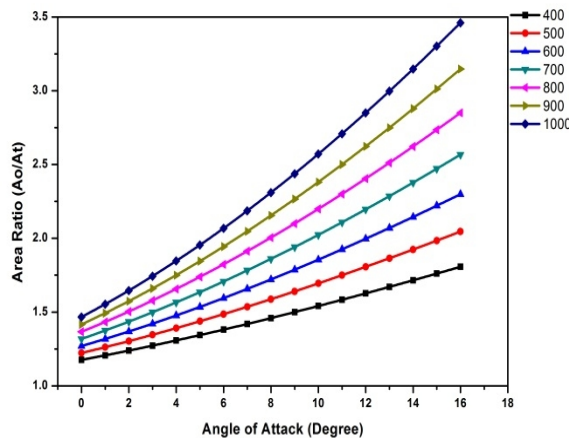
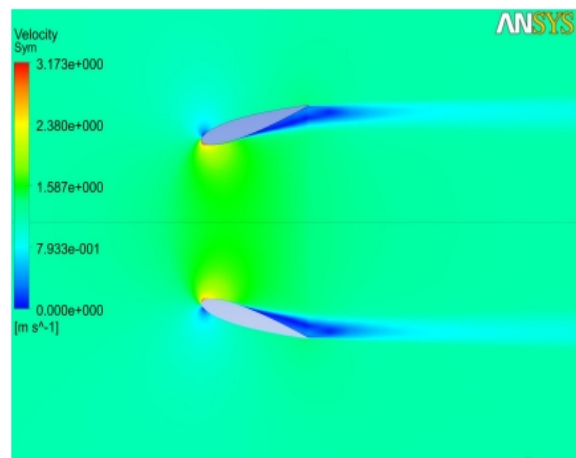
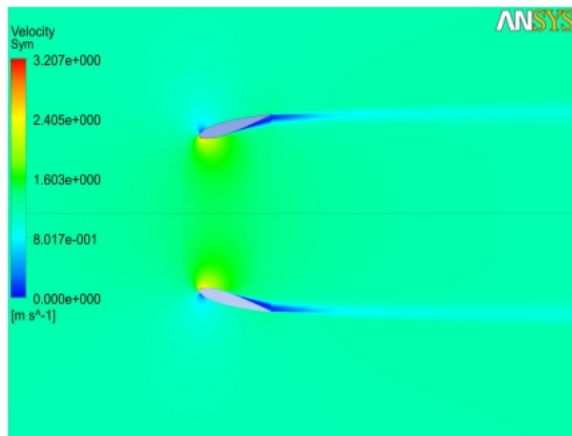
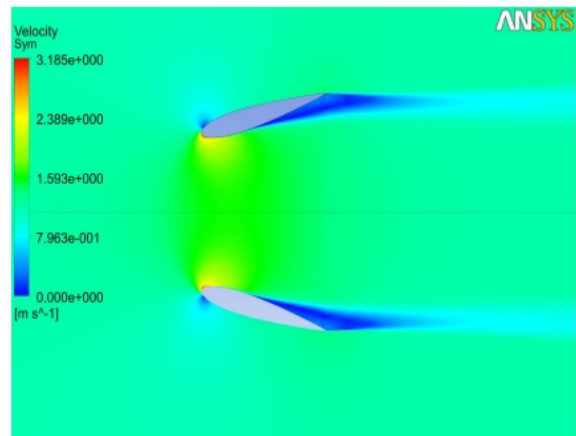
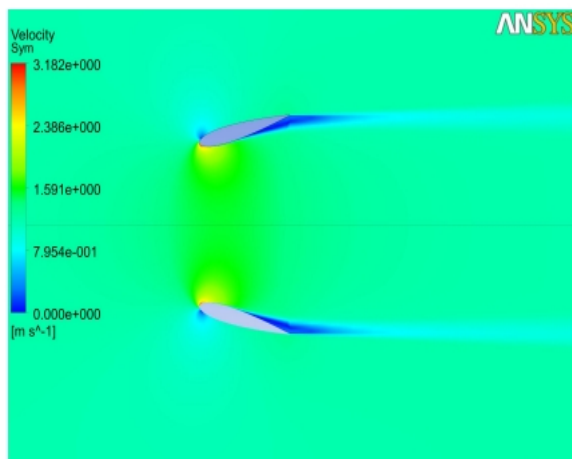
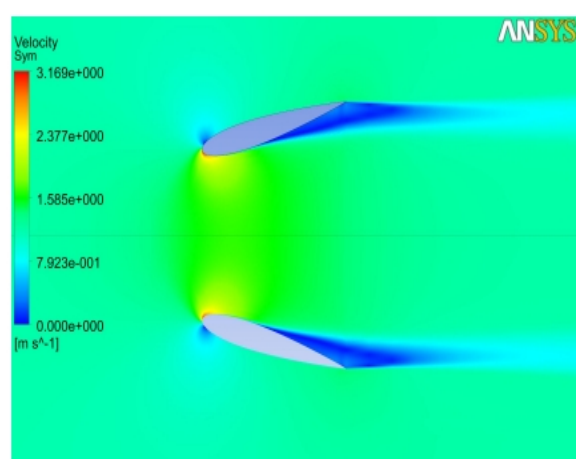


Figure 10. Maximum velocity vs angle of attack

**Figure 11.** Average velocity against angle of attack**Figure 14.** Coefficient of mass flow rate vs angle of attack**Figure 12.** Coefficient of velocity vs angle of attack**Figure 15.** Drag force vs angle of attack**Figure 13.** Mass flow rate at throat vs angle of attack**Figure 16.** Coefficient of drag force vs angle of attack

**Figure 17.** Area ratio vs angle of attack**Figure 20.** Velocity profile for 600mm & 16° attack angle**Figure 18.** Velocity profile for 400mm & 15° attack angle**Figure 21.** Velocity profile for 700mm & 16° attack angle**Figure 19.** Velocity profile for 500mm & 15° attack angle**Figure 22.** Velocity profile for 800mm & 16° attack angle

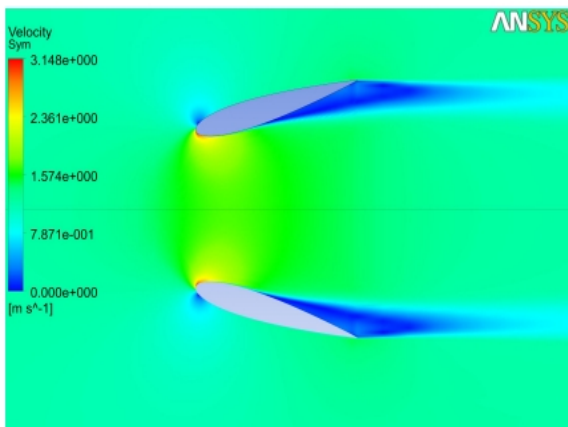


Figure 23.Velocity profile for 900mm & 16° attack angle

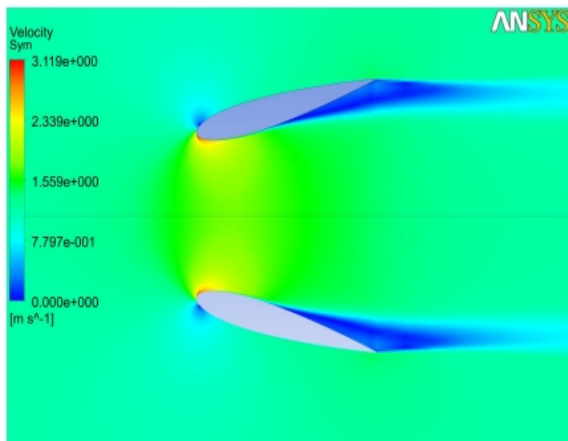


Figure 24.Velocity profile for 1000mm & 15° attack angle

Figures 18, 19, 20, 21, 22, 23 and 24 depict velocity profiles at 400mm length & 15 degree angle of attack, 500mm length & 15 degree angle of attack, 600mm length & 16 degree angle of attack, 700mm length & 16 degree angle of attack, 800mm length & 16 degree angle of attack, 900mm length & 16 degree angle of attack and 1000mm length & 15 degree angle of attack, respectively. Above mentioned figures give the in-depth view of the velocity profile which help to magnify the visualization of the reader inside the diffuser.

4. CONCLUSION

NACA 0015 airfoil has been investigated at different lengths and angles of attack to explore its potential for diffuser design. The following remarks are concluded:

1. Velocity in the diffuser increases with diffuser length and the angle of attack.

2. It has been observed that inlet velocity increases from 1.2 m/sec to 3.18 m/sec which is around 165 % increase in velocity.
3. Maximum velocity, average velocity and mass flow rate drops after 14 degree angle of attack, which is due to the stall angle.
4. The mass flow rate is the function of cross sectional area and velocity, it also drops a little after 14 degree angle of attack, due to stall angle.
5. Drag is an important parameter for commercial projects. Drag increases with length and angle. There is always a compromise that has to be made between maximum velocity and drag. Compromise on drag means a bigger support structure is needed to cater the drag which ultimately means more capital cost.

6. ACKNOWLEDGEMENTS

This research is financially supported by National Special Foundation for Ocean Commonweal (Grant No.200805040), S&T Program (Grant No.2008BAA15B06), Ocean Renewable Energy (Grants No.GHME2010GC02 & GHME2010GC03), '111 Project', Foundation from State Administration of Foreign Experts Affairs in China and Ministry of Education of China (Grant No.B07019).

7. REFERENCES

1. Betz, A., "Energieumsetzungen in Venturidusen", *Die Naturwissenschaften*, Vol. 17, No. 10 (1929), 160–164.
2. Sanuki, M., "Studies on biplane windvanes ventilator-tubes and cup anemometers", *Papers in meteorology and geophysics*, Vol. 1, No. 2 (1950), 27–290.
3. Iwasaki, M., "The experimental and theoretical investigation of windmills", *Reports of Research Institute for Applied Mechanics*, Vol. 2, No. 8 (1953), 181–229.
4. Rainbird, W. J., and Lilley, G. M., "A Preliminary Report on the Design and Performance of a Ducted Windmill" Report 102, (1956).
5. Kogan, A., and Seginer, A., "Shrouded Aerogenerator Design Study II, Axisymmetrical shroud performance", Department of Aeronautical Engineering, Technion, T.A.E. Report 32, (1963).
6. Kogan, A., and Seginer, A., "Final Report on Shroud Design" Department of Aeronautical Engineering, Technion, T.A.E. Report 32A, (1963).
7. Gilbert, B. L., and Foreman, K. M., "Experimental Demonstration of the Diffuser-Augmented Wind Turbine Concept", *Journal of Energy*, Vol. 3, No. 4 (1979), 235–240.
8. Gilbert, B. L., and Foreman, K. M., "Fluid Dynamics of Diffuser-Augmented Wind Turbines", *Journal of Energy*, Vol. 2, No. 6 (1978), 368–374.
9. Lewis, R. I., Williams, J. E., and Abdelghaffar, M. A., "A Theory and Experimental Investigation of Ducted Wind Turbines", *Wind Engineering*, Vol. 1, No. 2 (1977), 104–125.

10. Vries, O. D., "Fluid Dynamic Aspects of Wind Energy Conversion", *AGARDograph*, Vol. 243, (1979).
11. Phillips, D. G., Flay, R. G. J., and Nash, T. A., "Aerodynamic Analysis and Monitoring of the Vortec Seven Diffuser Augmented Wind Turbine" In Proceedings of the Annual Conference of the Institute of Professional Engineers NZ, Auckland, (1998), 20.
12. Nasir, M., Zhang, L., and Jawad, K., "Harnessing Ocean Energy by Tidal Current Technologies", *Research Journal of Applied Sciences, Engineering and Technology*, Vol. 4, No. 18 (2012), 3476-3487.
13. Nasir, M., Zhang, L., and Jawad, K., "CFD study of 2D model of diffuser for harnessing tidal energy", *Advanced Materials Research*, Vol. 482-484, (2012), 2270-2274.
14. Norimasa, S., Toshiaki S., Yoichi K., and Kaneko, K., "Development of Two-Way Diffuser for Tidal Energy Conversion System", *Renewable Energy*, Vol. 29, No. 10 (2004), 1757-1771.
15. Ohya, Y., Karasudani, T., Sakurai, A., Abe, K., and Inoue, M., "Development of a shrouded wind turbine with a flanged diffuser", *Journal of Wind Engineering and Industrial Aerodynamics*, Vol. 96, (2008), 524-539.
16. Karasudani, T., Fukamachi, N., Watanabe, K., and Ohya, Y., "Enhancement of Wind Speed in a Diffuser by Entrainment," Proc. of Japan Society of Fluid Mechanics 2001, JSFM, Japan, 587-588 (in Japanese).
17. Nasir, M., Zhang, L., and Jawad, K., "Diffuser Augmented Horizontal Axis Tidal Current Turbines", *Research Journal of Applied Sciences, Engineering and Technology*, Vol. 4, No. 18 (2012), 3522-3532.
18. Ansys CFX Solver Theory Guide.
<http://www1.ansys.com/customer/content/documentation/120/cfx/xthry.pdf>

Study of NACA 0015 for Diffuser Design in Tidal Current Turbine Applications

TECHNICAL NOTE

N. Mehmood^a, Z. Liang^a, J. Khan^b

^a Deepwater Engineering Research Center, Harbin Engineering University, 150001, Harbin, China

^b College of Shipbuilding Engineering, Harbin Engineering University, 150001, Harbin, China

PAPER INFO

Paper history:

Received 16 July 2012

Received in revised form 11 August 2012

Accepted 30 August 2012

چکیده

انرژی جزر و مد قابل پیش بینی ترین شکل از انرژی های تجدید پذیر است. انرژی جزر و مد به کمک سدبنده، حصار و فن آوری های امروزی مهار شده است. این پژوهش، افزودن یک دیفیوزر به یک توربین جزر و مدی است که بر بهره برداری از انرژی جنبشی جریان جزر و مدی متوجه شده است. قادرت تولید شده توسط توربین جزر و مدی به دلیل وجود یک رابطه توان سوم بین قدرت و سرعت جریان است. افزایش جزئی در سرعت جریان به میزان قابل توجهی قدرت خروجی را افزایش می دهد. دیفیوزر دستگاهی است که می تواند محرك سرعت جریان باشد. ترکیبی از یک دیفیوزر با یک توربین، می تواند بهره وری از توربین جزر و مدی را افزایش دهد. بسیاری از گروه های تحقیقاتی در حال سرمایه گذاریهای قابل توجهی از لحاظ زمانی و منابع مالی در این حوزه در حال ظهور هستند. نتایج محدودی از ترکیب یک دیفیوزر با یک توربین جزر و مدی موجود است که این هم به دلایل جدید بودن موضوع مورد بررسی، بزرگ و پژوهیه بودن تحقیقات و مشکلات نصب، هزینه راه اندازی و مسائل اخلاقی دیگر می باشند. هدف از این مقاله این است که به مطالعه ایرفویل NACA 0015 برای طراحی دیفیوزر برای توربین جزر و مدی پردازد. شبیه سازی عددی دیفیوزر که به بررسی سرعت و سرعت جریان توده در گلوگاه می پردازد، انجام شده است. همچنین نیروی دراگ، برای مدل های مختلف دیفیوزر NACA 0015 محاسبه شده است.

doi: 10.5829/idosi.ije.2012.25.04c.12